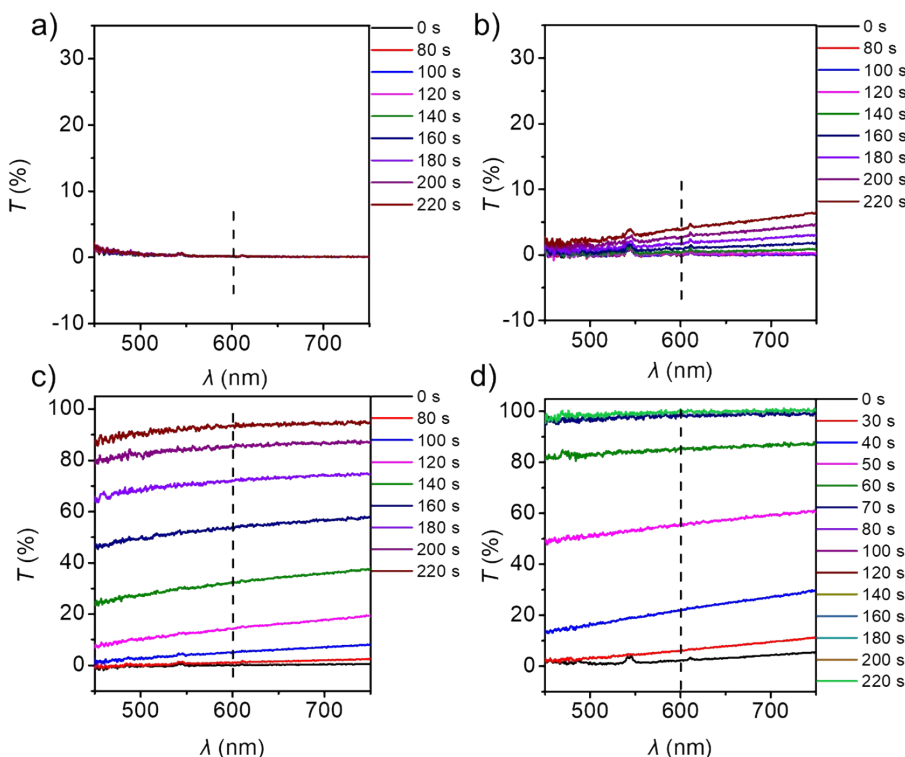


**Supporting information**

**Low-voltage and Wide-tuning-range  $\text{SiO}_2$ /Aniline Electrically Responsive Photonic Crystal  
Fabricated by Solvent Assisted Charge Separation**

*Guangyang Bao, Wenyuan Yu, Qianqian Fu, Jianping Ge\**



**Figure S1.** Time evolution of transmittance for  $\text{SiO}_2$  colloidal dispersions ( $f_{\text{SiO}_2} = 2\%$ ) in a) aniline (ANI), b) 1,2-dichlorobenzene (DCB), c) anisole (ANIS) and d) toluene (TOL).

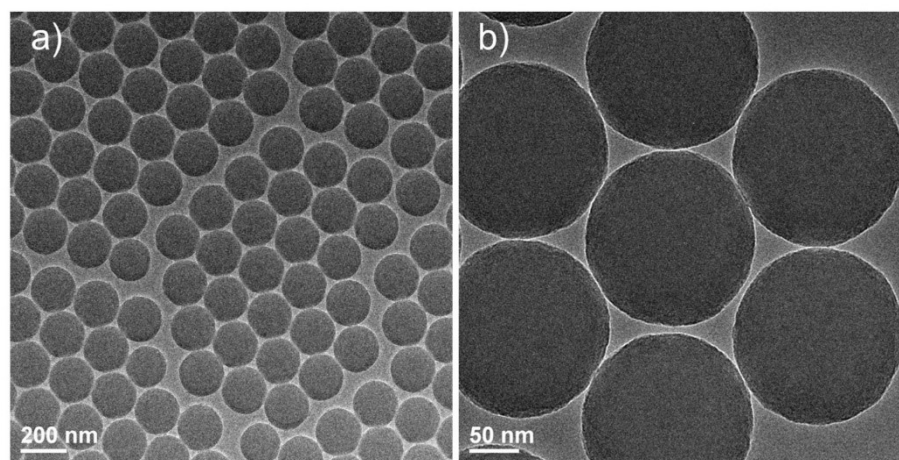


**Figure S2.** a, b) TEM images of monodisperse  $\text{SiO}_2$  particles.

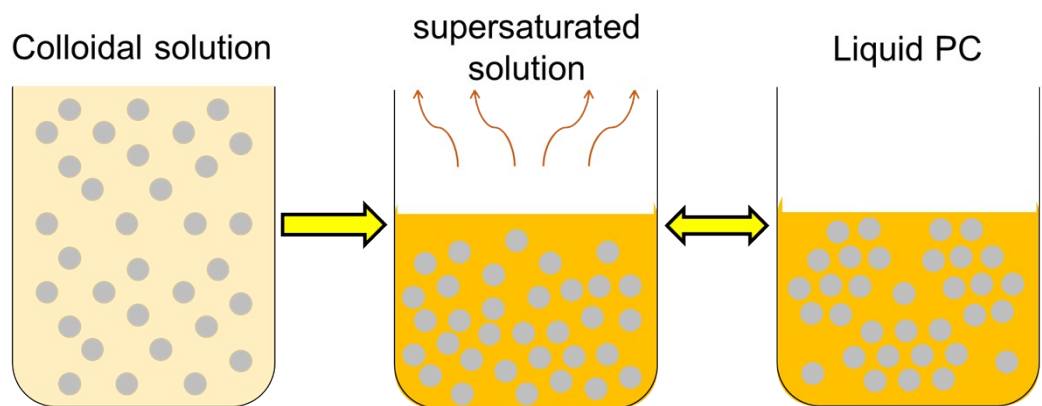


**Figure S3.** Preparation of liquid PCs via evaporation-induced supersaturation of colloidal particles and spontaneous precipitation of colloidal crystals.

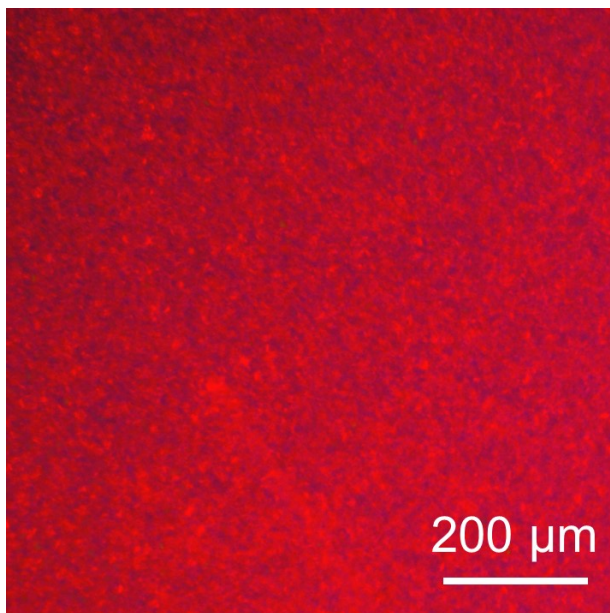


**Figure S4.** Optical microscopic image of  $\text{SiO}_2/\text{ANI}$  liquid PC.

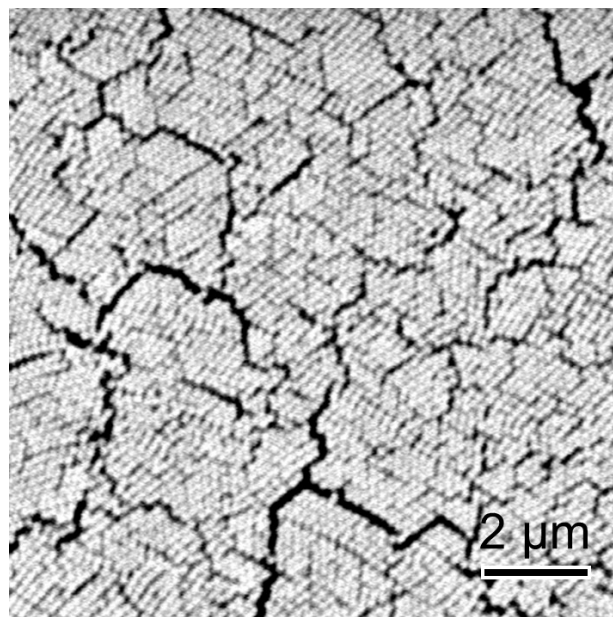


**Figure S5.** SEM image of  $\text{SiO}_2$  PC film after complete evaporation of solvent in liquid PC.

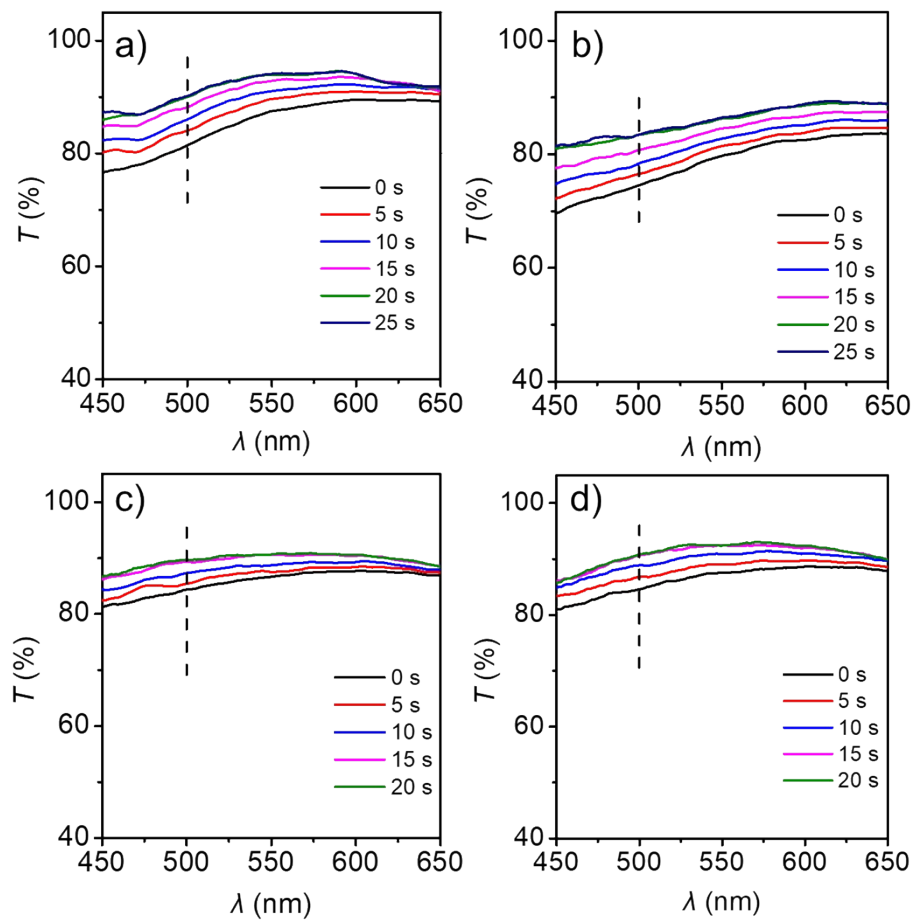


**Figure S6.** Time evolution of transmission spectra for  $\text{SiO}_2$  colloidal dispersions ( $f_{\text{SiO}_2} = 2\%$ ) in a) isopropanol (IPA), b) EtOH, c) DMF-EtOH, and d) PCb-EtOH under external field of 2 V.

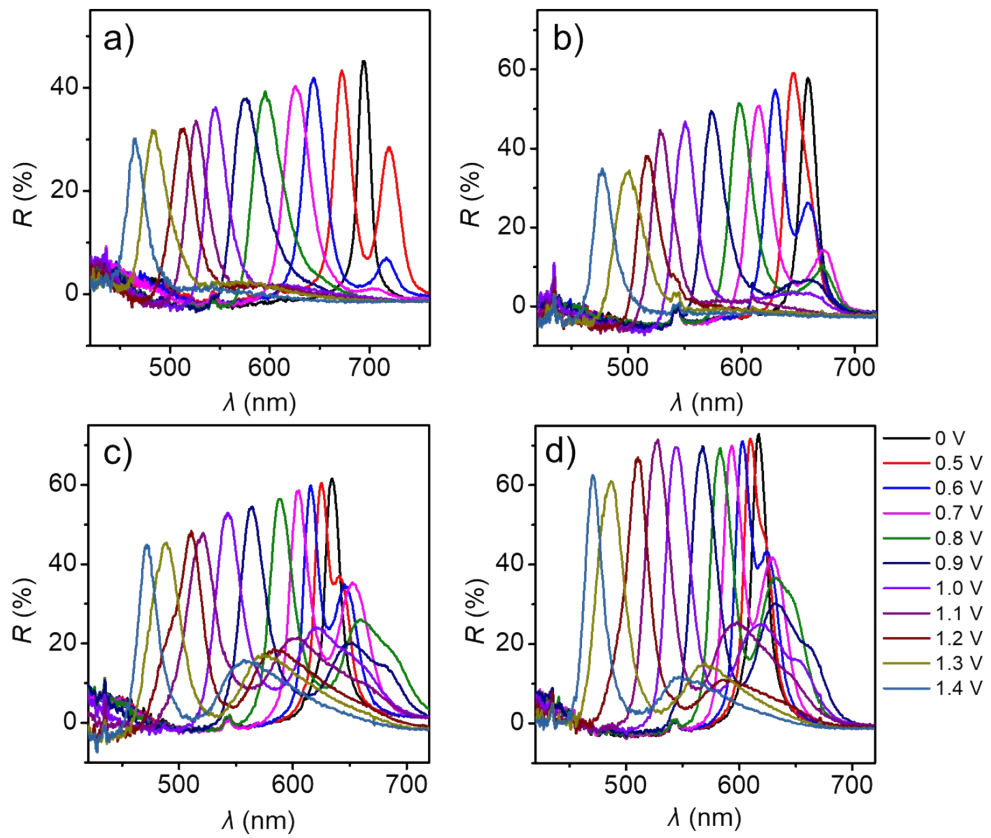


**Figure S7.** Reflection spectra of  $\text{SiO}_2/\text{ANI}$  ERPCs with particle volume fraction of a) 18%, b) 22%, c) 25%, and d) 30% as the applied voltage was increased from 0 to 1.4 V.

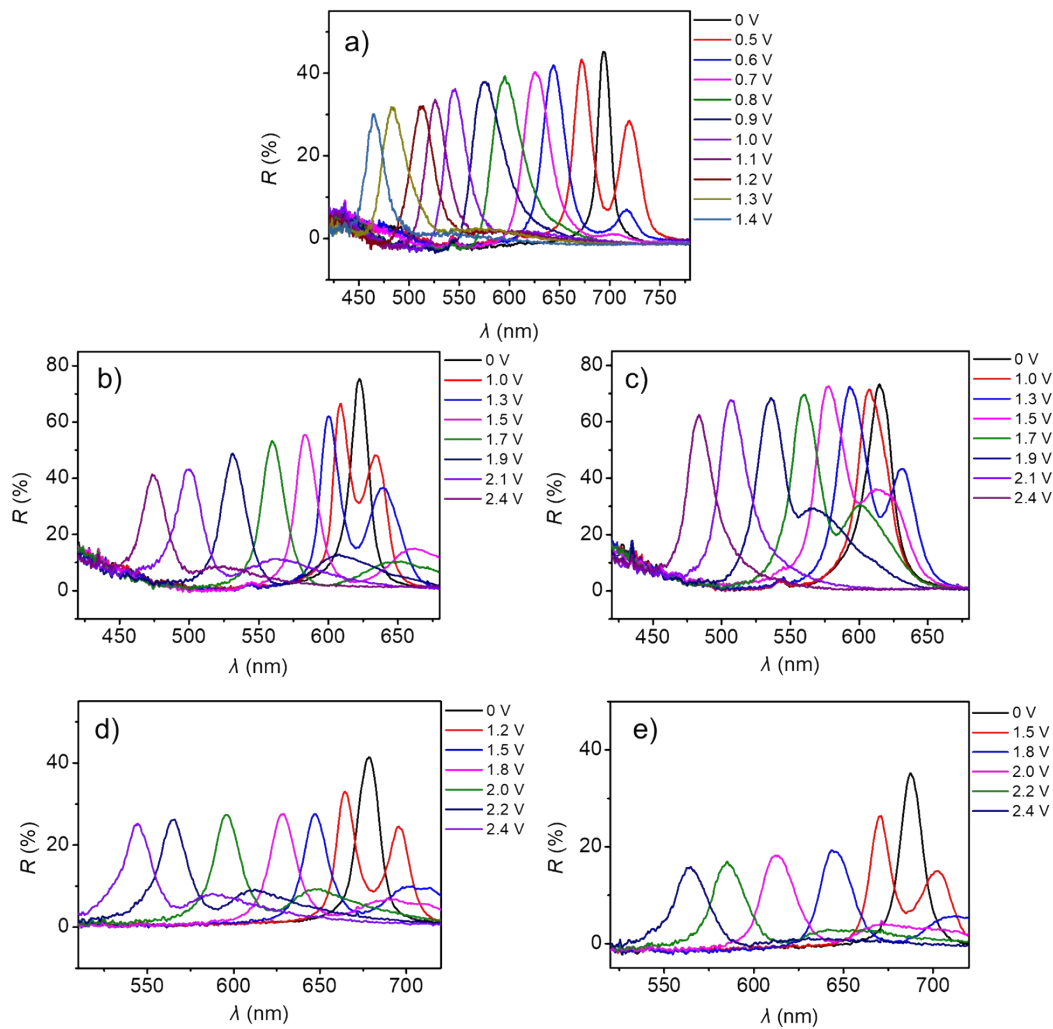


**Figure S8.** The reflection spectra of a)  $\text{SiO}_2/\text{ANI}$ , b)  $\text{SiO}_2/\text{IPA}$ , c)  $\text{SiO}_2/\text{EtOH}$ , d)  $\text{SiO}_2/\text{DMF}$ , and e)  $\text{SiO}_2/\text{PCb}$  ERPCs under various applied voltages.

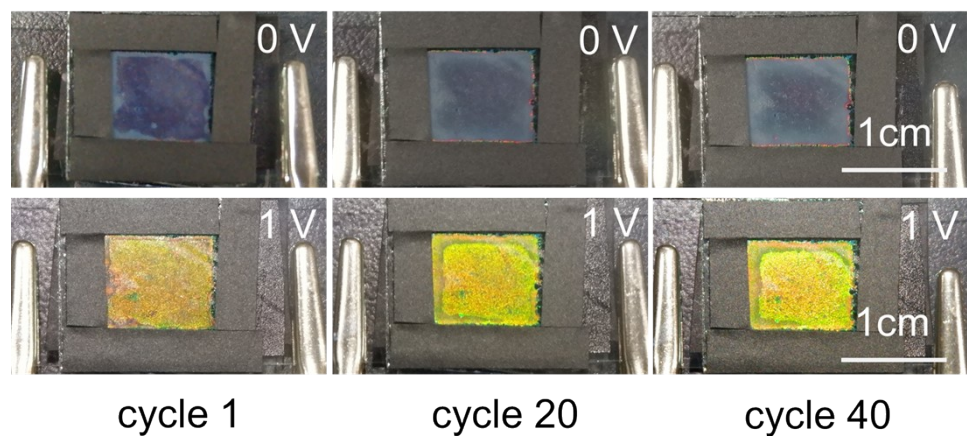


**Figure S9.** Digital photos of  $\text{SiO}_2/\text{ANI}$  ERPC as the electric field was switched on (1 V) or off (0 V) for multiple cycles.

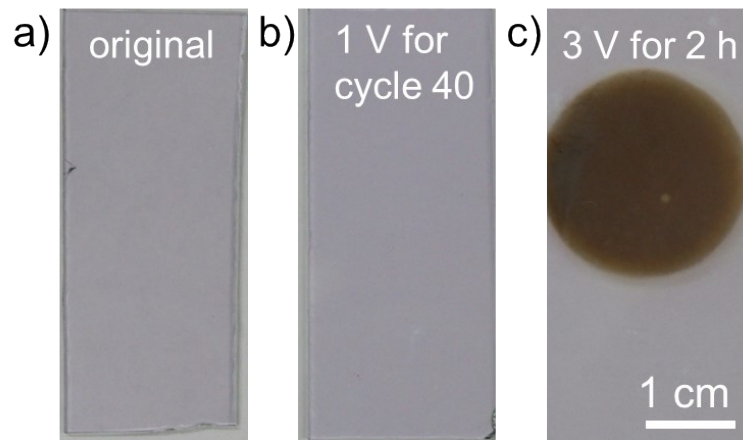


**Figure S10.** Digital photos of a) original ITO glass, b) ITO cathode of  $\text{SiO}_2/\text{ANI}$  ERPC under 1 V for cycle 40, and c) ITO cathode of  $\text{SiO}_2/\text{PCb}$  ERPC under 3 V for 2 h.

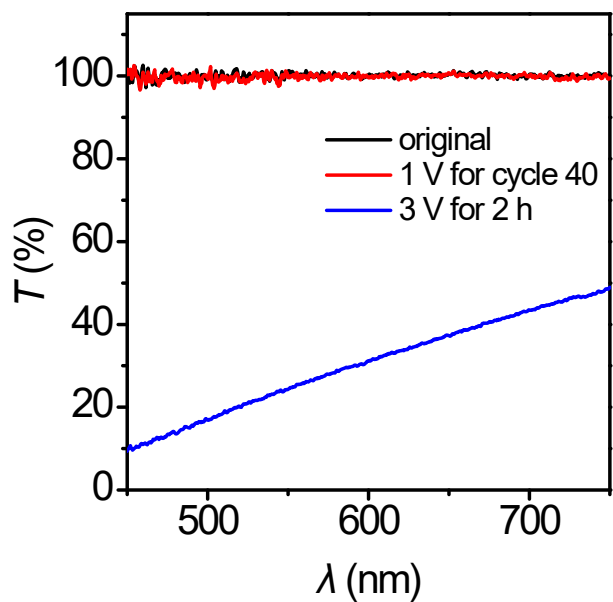


**Figure S11.** Transmittance spectra of a) original ITO glass, b) ITO cathode of  $\text{SiO}_2/\text{ANI}$  ERPC under 1 V for cycle 40, and c) ITO cathode of  $\text{SiO}_2/\text{PCb}$  ERPC under 3 V for 2 h.

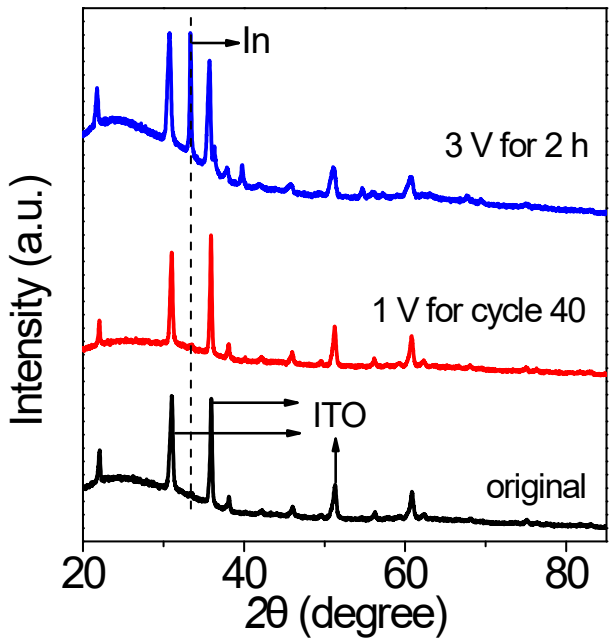


**Figure S12.** XRD spectra of a) original ITO glass, b) ITO cathode of  $\text{SiO}_2/\text{ANI}$  ERPC under 1 V for cycle 40, and c) ITO cathode of  $\text{SiO}_2/\text{PCb}$  ERPC under 3 V for 2 h.

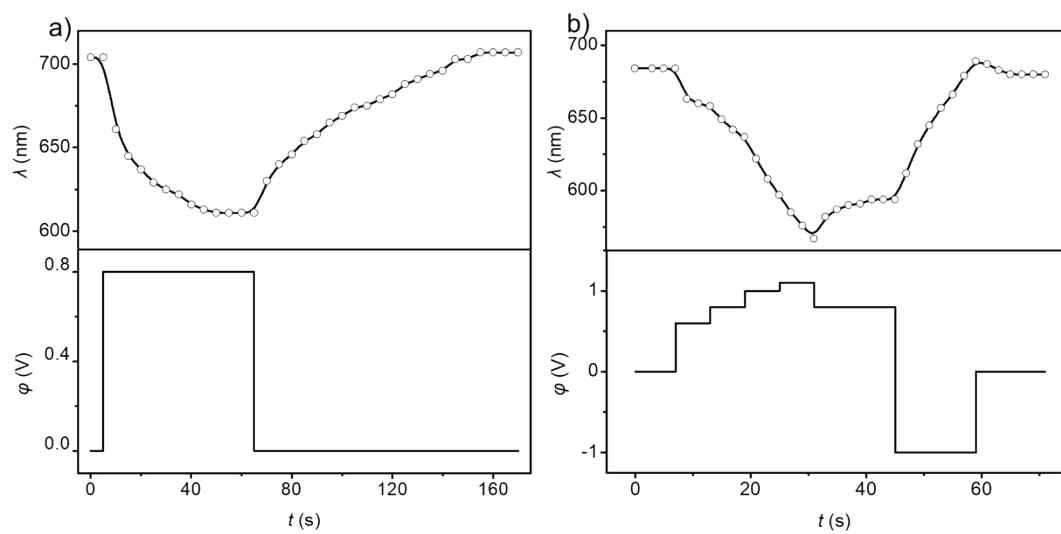


**Figure S13.** Time evolution of reflection wavelength of  $\text{SiO}_2/\text{ANI}$  ERPC during the switching of structural colors, which were realized by a) applying and removing the electric field directly and b) applying a step-rising and a reverse potential.

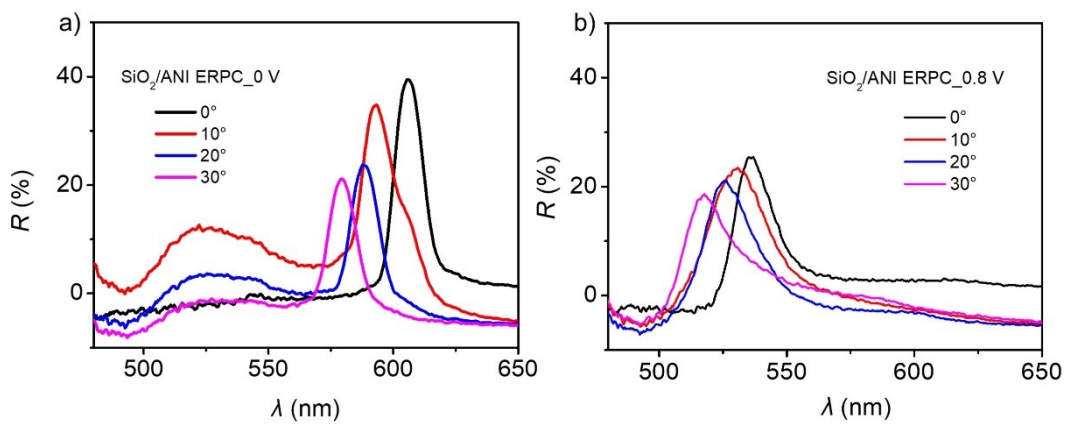


**Figure S14.** The angular dependent reflection spectra of  $\text{SiO}_2/\text{ANI}$  ERPC at a) 0 V and b) 0.8 V, where the incident angle was fixed at  $0^\circ$  and the reflected angle was changed from  $0^\circ$  to  $30^\circ$ .

**Table S1.** Assessment of zeta potential ( $\zeta$ ) of SiO<sub>2</sub> particles in different solvents by viscosity ( $\eta$ ) and dielectric constant ( $\epsilon$ ) of the solvent, and the changing speed of transmittance rising ( $dr_{T.R.}/dt$ ) under external field of 2 V.

Colloidal dispersion (f <sub>SiO<sub>2</sub></sub> =2%)	dr <sub>T.R.</sub> /dt	$\eta$ (mPa·s)	$\epsilon$	$\zeta/C_1C_2$ (mV)
SiO <sub>2</sub> /ANI	0.0271	4.40	7.06	0.0169
SiO <sub>2</sub> /IPA	0.0478	2.43	18.30	0.0064
SiO <sub>2</sub> /EtOH	0.0490	1.19	25.70	0.0023
SiO <sub>2</sub> /DMF-EtOH	0.0652	1.00*	32.31**	0.0020
SiO <sub>2</sub> /PCb-EtOH	0.0660	1.69*	51.68**	0.0022

\* The viscosities of the mixing solvents were tested by the viscometer

\*\* The dielectric constants of the mixing solvents were estimated by the equation:  $\epsilon_{mix}=f_1\epsilon_1+f_2\epsilon_2$ , where f and  $\epsilon$  denote to the volume fraction and the dielectric constant of the component.

**Table S2.** The center-to-center distance (D) and the surface-to-surface distance (D-d) of the neighboring particles in **SiO<sub>2</sub>/ANI ERPC** calculated by the measured reflection wavelength ( $\lambda$ ), the effective refractive index ( $n_e$ ), and the average diameter of the SiO<sub>2</sub> particles (171 nm).

<b>f<sub>SiO<sub>2</sub></sub></b>	<b>λ (nm)</b>	<b>n<sub>e</sub></b>	<b>D (nm)</b>	<b>D-d (nm)</b>
18%	694	1.5666	271	100
22%	659	1.5614	258	87
25%	634	1.5575	249	78
30%	617	1.5510	244	72

**Table S3.** Comparison of the chemical composition, the onset working potential, the maximum working potential, and the corresponding reflection wavelength changes for the various electrophoretic ERPCs in literature works and this work.

	Particles	$d_p$ (nm)	$f_p$ (%)	Solvent	$\phi$ (V)	$\Delta\lambda$ (nm)	Reference
1	Fe <sub>3</sub> O <sub>4</sub> @SiO <sub>2</sub>	150	25*	PCb	4.0	165	Adv. Mater. 2010, 22, 4973
2	sulfonated PS	178	22.1	H <sub>2</sub> O	-1.8	100	Adv. Mater. 2010, 22, 4494
3	ZnS@SiO <sub>2</sub>	120	>4.8	H <sub>2</sub> O	3.4	190	Adv. Mater. 2012, 24, 6438
4	PMMA-co-PS	137	/	H <sub>2</sub> O	3.5	259	J. Mater. Chem. C, 2013, 1, 5791
5	PS	138	/	H <sub>2</sub> O	3.2	150	Adv. Opt. Mater. 2014, 2, 535
6	PS	138	/	H <sub>2</sub> O	3.2	165	Appl. Phys. Lett. 2014, 104, 051104
7	Fe <sub>3</sub> O <sub>4</sub> @C	110 or 130	18*	PCb	2.6	150	RSC Adv., 2016, 6, 100167
8	Fe <sub>3</sub> O <sub>4</sub> @SiO <sub>2</sub>	150	12.6	PCb	2.0	210	J. Alloy. Comp. 2016, 654, 251
9	Fe <sub>2</sub> O <sub>3</sub> @SiO <sub>2</sub>	127	14	PCb	4.0	70	Adv. Opt. Mater. 2017, 5, 1600838
10	CeO <sub>2</sub> @SiO <sub>2</sub>	175	17.5	PCb	3.5	154	Adv. Funct. Mater. 2018, 28, 1804628
11	PtBMA	200	40*	IPG-HC-AOT	4.0	114	ACS Appl. Mater. Interfaces 2018, 10, 11776
12	Fe <sub>3</sub> O <sub>4</sub> @SiO <sub>2</sub>	145	15	PCb	3.0	144	RSC Adv., 2019, 9, 498
13	PMMA-PtBMA	200	40*	IPG-HC-AOT	4.0	121	Adv. Opt. Mater. 2021, 9, 2100833
14	HPO-SiO <sub>2</sub>	145	17.6	DCB-AOT	1.7	181	Adv. Opt. Mater. 2022, 10, 2201188
15	SiO <sub>2</sub>	171	18	ANI	<b>1.4</b>	<b>230</b>	this work

\* These  $f_p$  values referred to the weight percentages of colloidal particles

**Table S4.** The center-to-center distance ( $D$ ) of the neighboring particles, the amount of compression lattice ( $1-D/D_0$ ) and the normalized reflection intensity ( $R/R_0$ ) of the **SiO<sub>2</sub>/ANI ERPC** calculated by the measured reflection wavelength ( $\lambda$ ) and the reflection intensity ( $R$ ) under different voltage ( $\varphi$ ), and the effective refractive index ( $n_e$ ).

$\varphi$ (V)	$\lambda$ (nm)	R (%)	$n_e$	D (nm)	1-D/D <sub>0</sub> (%)	R/R <sub>0</sub> (%)
0	694	46	1.5666	271	0	100
0.5	672	44	1.5666	263	3.2	96
0.6	644	42	1.5666	252	7.2	91
0.7	625	41	1.5666	244	10	89
0.8	595	39	1.5666	233	14.3	85
0.9	575	38	1.5666	225	17.1	83
1	545	36	1.5666	213	21.5	78
1.1	526	34	1.5666	206	24.2	74
1.2	512	32	1.5666	200	26.2	70
1.3	484	31	1.5666	189	30.3	67
1.4	464	30	1.5666	181	33.1	65

**Table S5.** The center-to-center distance ( $D$ ) of the neighboring particles, the amount of compression lattice ( $1-D/D_0$ ) and the normalized reflection intensity ( $R/R_0$ ) of the **SiO<sub>2</sub>/IPA ERPC** calculated by the measured reflection wavelength ( $\lambda$ ) and the reflection intensity ( $R$ ) under different voltage ( $\varphi$ ), and the effective refractive index ( $n_e$ ).

$\varphi$ (V)	$\lambda$ (nm)	R (%)	$n_e$	D (nm)	1-D/D <sub>0</sub> (%)	R/R <sub>0</sub> (%)
0	622	76	1.3944	273	0	100
1	609	66	1.3944	267	2.1	86.8
1.3	601	62	1.3944	264	3.4	81.6
1.5	584	56	1.3944	256	6.1	73.7
1.7	560	54	1.3944	246	10	71.1
1.9	531	49	1.3944	233	14.6	64.5
2.1	498	44	1.3944	219	20	57.9
2.4	474	41	1.3944	208	23.8	53.9

**Table S6.** The center-to-center distance ( $D$ ) of the neighboring particles, the amount of compression lattice ( $1-D/D_0$ ) and the normalized reflection intensity ( $R/R_0$ ) of the **SiO<sub>2</sub>/EtOH ERPC** calculated by the measured reflection wavelength ( $\lambda$ ) and the reflection intensity ( $R$ ) under different voltage ( $\varphi$ ), and the effective refractive index ( $n_e$ ).

$\varphi$ (V)	$\lambda$ (nm)	R (%)	$n_e$	D (nm)	1-D/D <sub>0</sub> (%)	R/R <sub>0</sub> (%)
0	615	74	1.378	273	0	100
1	608	72	1.378	270	1.1	97
1.3	594	72	1.378	264	3.4	97
1.5	577	72	1.378	256	6.2	97
1.7	560	70	1.378	249	8.9	95
1.9	536	68	1.378	238	12.8	92
2.1	507	68	1.378	225	17.6	92
2.4	484	63	1.378	215	21.3	85

**Table S7.** The center-to-center distance ( $D$ ) of the neighboring particles, the amount of compression lattice ( $1-D/D_0$ ) and the normalized reflection intensity ( $R/R_0$ ) of the **SiO<sub>2</sub>/DMF ERPC** calculated by the measured reflection wavelength ( $\lambda$ ) and the reflection intensity ( $R$ ) under different voltage ( $\varphi$ ), and the effective refractive index ( $n_e$ ).

$\varphi$ (V)	$\lambda$ (nm)	R (%)	$n_e$	D (nm)	1-D/D <sub>0</sub> (%)	R/R <sub>0</sub> (%)
0	678	42	1.4354	289	0	100
1.2	664	33	1.4354	283	2.1	79
1.5	647	28	1.4354	276	4.6	67
1.8	628	28	1.4354	268	7.4	67
2	596	28	1.4354	254	12.1	67
2.2	565	26	1.4354	241	16.7	62
2.4	544	25	1.4354	232	19.8	60

**Table S8.** The center-to-center distance ( $D$ ) of the neighboring particles, the amount of compression lattice ( $1-D/D_0$ ) and the normalized reflection intensity ( $R/R_0$ ) of the **SiO<sub>2</sub>/PCb ERPC** calculated by the measured reflection wavelength ( $\lambda$ ) and the reflection intensity ( $R$ ) under different voltage ( $\varphi$ ), and the effective refractive index ( $n_e$ ).

$\varphi$ (V)	$\lambda$ (nm)	R (%)	$n_e$	D (nm)	1-D/D <sub>0</sub> (%)	R/R <sub>0</sub> (%)
0	687	35	1.4272	295	0	100
1.5	671	26	1.4272	288	2.3	74
1.8	644	19	1.4272	276	6.3	54
2	613	19	1.4272	263	10.8	51
2.2	584	17	1.4272	251	15	49
2.4	564	16	1.4272	242	17.9	46